Biophysical Chemistry 203–204 (2015) 33–40

Contents lists available at ScienceDirect

Biophysical Chemistry

journal homepage: http://www.elsevier.com/locate/biophyschem

A neglected modulator of insulin-degrading enzyme activity and conformation: The pH

Giuseppe Grasso [a,*], Cristina Satriano [a], Danilo Milardi [b]

[a] Dipartimento di Scienze Chimiche, Università degli Studi di Catania, Viale Andrea Doria 6, 95125 Catania, Italy
[b] Istituto Biostrutture e Bioimmagini, CNR, Via P. Gaifami 18, 95126 Catania, Italy

HIGHLIGHTS

- IDE is present in different cellular environments experiencing different pH values.
- IDE conformation and activity have been investigated at various pH values.
- IDE is monomeric and inactive at acidic pH, while it is active at neutral and basic pH.
- Insulin cryptic peptides produced by IDE are different at different pH values.

GRAPHICAL ABSTRACT

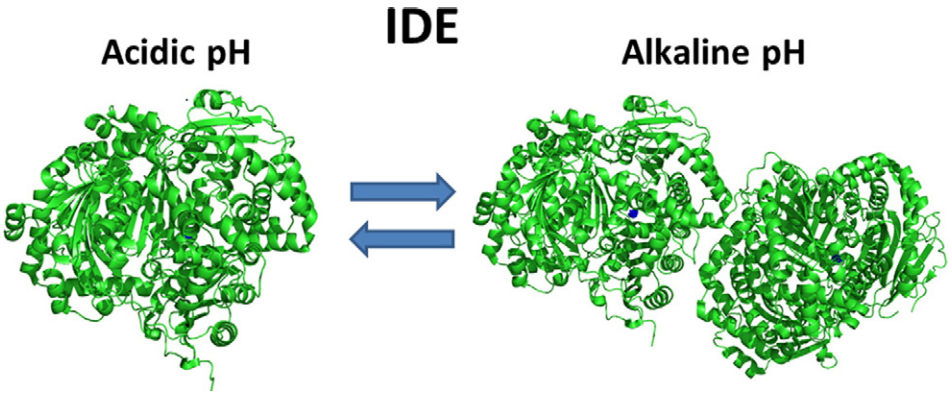

ARTICLE INFO

Article history:
Received 30 March 2015
Received in revised form 19 May 2015
Accepted 21 May 2015
Available online 27 May 2015

Keywords:
IDE
Mass spectrometry
Surface plasmon resonance
Acidity
Enzyme
Activity

ABSTRACT

Insulin-degrading enzyme (IDE), a ubiquitously expressed zinc metalloprotease, has multiple activities in addition to insulin degradation and its malfunction is believed to connect type 2 diabetes with Alzheimer's disease. IDE has been found in many different cellular compartments, where it may experience significant physio-pathological pH variations. However, the exact role of pH variations on the interplay between enzyme conformations, stability, oligomerization state and catalysis is not understood.

Here, we use ESI mass spectrometry, atomic force microscopy, surface plasmon resonance and circular dichroism to investigate the structure–activity relationship of IDE at different pH values. We show that acidic pH affects the ability of the enzyme to bind the substrate and decrease the stability of the protein by inducing an α-helical bundle conformation with a concomitant dissociation of multi-subunit IDE assemblies into monomeric units and loss of activity. These effects suggest a major role played by electrostatic forces in regulating multi-subunit enzyme assembly and function. Our results clearly indicate a pH dependent coupling among enzyme conformation, assembly and stability and suggest that cellular acidosis can have a large effect on IDE oligomerization state, inducing an enzyme inactivation and an altered insulin degradation that could have an impact on insulin signaling.

1. Introduction

Insulin-degrading enzyme (IDE) is a zinc metalloprotease of the M16 family whose activity and functions have been correlated with

* Corresponding author at: Dipartimento di Scienze Chimiche, Università di Catania, Viale Andrea Doria 6, 95125 Catania, Italy.
E-mail address: grassog@unict.it (G. Grasso).

http://dx.doi.org/10.1016/j.bpc.2015.05.010
0301-4622/

various diseases, such as diabetes [1], cancer [2] and Alzheimer's disease (AD) [3]. In the attempt to conveniently modulate IDE activity, in recent years many studies have been conducted in order to assess the molecular details of the IDE interaction with various substrates and modulators [4–9]. In this perspective, the search of possible inhibitors as well as activators of IDE has risen, according to the strategy of decreasing [10] or increasing [11] the proteolysis of, respectively, insulin and Aβ peptides after they are produced. Indeed, considerable evidence suggests that IDE inhibitors may hold therapeutic value, particularly for type 2 diabetes and other disorders involving impaired insulin signaling [12], while IDE activators could be used as possible drugs aiming at lowering Aβ levels in AD [13]. Moreover, the effect that other experimental factors such as oligomerization state [14–16], presence of metal ions [17–20] and oxidative stress [21–23] can have on IDE activity has also been widely investigated.

In this scenario, it is important to highlight that, although IDE is primarily cytosolic [24], other cellular localizations have been observed, including peroxisomes [25,26] and mitochondria [27], while a small fraction of the enzyme have been also found on the plasma membrane of Chinese hamster ovary (CHO) cells [28]. Moreover, in a recent study, it was reported that IDE exists primarily on the surface of human cerebrovascular endothelial cells and this form of the enzyme seems to be the main responsible for degrading Aβ peptides [29]. This wide distribution of IDE localization means that the enzyme can experience different environmental pH values. Indeed, although a comprehensive understanding of how cellular organelles maintain their different pH values does not exist, it is well known that their distinctive pH values are essential to their function and that are set and maintained by a balance between ion pumps, leaks, and internal ionic equilibria [30]. The presence of different pH values has been widely recognized to play an important role in Aβ aggregation and fibrillogenesis [31], and Aβ production occurs in the slightly acidic environments of the endosomes (pH 5–6.5) and the lysosomes (pH 4–5). Analogously, insulin degradation can occur intra- and extracellularly and IDE has been reported to be responsible for this hormone catabolism at non-acidic pH [24]. Indeed, it has been already reported that at a pH of 6 or less, IDE has little proteolytic activity and thus, in acidified vesicles, insulin degradation must occur by other enzymatic mechanisms. However, IDE seems to function not only as an insulin degradative enzyme but also as an intracellular insulin binding and regulatory protein. In this perspective, insulin–IDE interaction could be important for the insulin signal transduction pathway and for mediating the intermediate effects of insulin on fat and protein turnover [24].

Here, we have applied CD, AFM, SPR and MS analytical tools in order to assess the effect of pH on IDE conformation/oligomerization state, as well as on binding capability and activity toward insulin. Specifically, we not only investigated the narrow range from pH ~ 5 to pH ~ 8, strictly related to physio-pathological environmental conditions relevant for the enzyme, but also considered the extremely acid (pH = 3) and basic (pH = 10) values, the latter has been considered for several reasons. Firstly, the IDE behavior at the extreme pH values was scrutinized for the methodological approach, in order to make the modifications occurring gradually from acid to alkaline pH values more visible. Secondly, the investigation of extreme pH values is also useful to give an insight in the overall enzyme thermodynamic stability [32]. Finally, it is important to note that IDE is expressed in several different tissues as well as being located in various cellular compartments [33] that experience different pH values. The latter has been reported to reach values as low as 4.7 in lysosome [34] or as high as 10 at the pancreatic duct just below the pylorus [35]. Results show that at acidic pH IDE has a conformation that stabilizes the monomeric form and is still capable to bind insulin molecules at one anchoring site but loses its ability to degrade the hormone.

2. Materials and methods

2.1. Enzyme assays and mass spectrometric measurements

Wild type, human, unlabeled IDE was purchased from Giotto Biotech S.r.l. Via Madonna del Piano, 6-50019 Sesto Fiorentino (FI) — Italy and its activity was verified by carrying out enzymatic digestion of insulin solutions according to the experimental procedure previously reported [15]. Methanol (MeOH), HEPES buffer and all chemicals used were purchased from Sigma-Aldrich. ZIPTIP C18 was purchased from Millipore (Milan, Italy). IDE enzymatic assays were carried out by incubating the enzyme solution (20 nM) at 37 °C with insulin solution at a concentration of 10 μM. After purification with ZIPTIP C18, 3 μL of the resulting solution was mixed with 50 μL of water and 50 μL of MeOH and injected into the mass spectrometer at 5 μL/min. ESI-MS experiments were performed by using a Finnigan LCQ DECA XP PLUS ion trap spectrometer operating in the positive ion mode and equipped with an orthogonal ESI source (Thermo Electron Corporation, Madison, WI, USA). Sample solutions were injected into the ion source using nitrogen as the drying gas. The mass spectrometer operated with a capillary voltage of 46 V and a capillary temperature of 250 °C, while the spray voltage was 4.3 kV.

2.2. Atomic force microscopy (AFM)

For atomic force microscopy (AFM), IDE solutions (150 nM) were allowed to adsorb at room temperature on freshly cleaved muscovite mica (Ted Pella, Inc.). After 5 min, the mica surface was briefly washed with 100 μL ultrapure water, dried under a gentle nitrogen stream and immediately imaged. A Cypher AFM instrument (Asylum Research, Oxford Instruments, Santa Barbara, CA) operating in AC-mode and equipped with a scanner at XY scan range of 30/40 μm (closed/open loop) was used. Silicon tetrahedral tips mounted on rectangular 30-μm long cantilevers were purchased from Olympus (AT240TS, Oxford Instruments). The probes had nominal spring constants of 2 N/m and driving frequencies of 70 kHz. A number of images covering 1 to 2 μm^2 surfaces were scanned and the lengths of particles were measured using a freehand tool in the MFP-3DTM offline section analysis software. The same tool was used to measure cross sections of particles. Statistical analysis was done with the Origin 8.3 software package.

2.3. Circular dichroism spectroscopy

Far-UV CD spectra of IDE were recorded with a Jasco J-810 spectropolarimeter equipped with a Peltier thermally controlled cuvette holder (JASCO PTC-348). All measurements were performed at 25 °C unless specified. IDE concentrations used in CD experiments were in the range of 1–2 μM. CD spectra were recorded using a 0.1-cm path length quartz cuvette, from 260 to 190 nm, at 0.1 nm data pitch, 50 nm/min, with a response time of 2 s. All spectra, corresponding to an average of 10 scans, were base-line-corrected by subtracting the signal of the buffer from the CD of the sample. CD curves were recorded in 5 mM of HEPES buffer and the pH was adjusted by adding NaOH or H_2SO_4. The thermally-induced unfolding of IDE was studied by monitoring the CD signal at 222 nm upon increasing the temperature from 20 to 80 °C (heating rate = 1 °C/min). The melting temperatures were calculated from fitting the normalized CD_{222} signals by a sigmoidal curve.

2.4. Surface plasmon resonance (SPR)

Surface plasmon resonance (SPR) measurements were carried out on a SensiQ Pioneer instrument, and all reagents used were from Sigma. IDE was immobilized on a COOH5 biosensor chip from ICx Nomadics (Oklahoma City, USA). Briefly, covalent immobilization was obtained by amine coupling of the lysine-free amino groups and terminal

amines of the protein, as described elsewhere [36–38]. Particularly, 400 μL of IDE solution at 100 μg/mL in 10 mM acetate buffer, pH 3.8, was used for the immobilization on a previously activated surface having reactive succinimide ester groups obtained by using 1-ethyl-3-(3-dimethylaminopropyl)carbodiimide (EDC) and N-hydroxysuccinimide (NHS) solution, freshly prepared ((EDC) = 0.4 M, (NHS) = 0.1 M). NaOH or HCl 1 mM was used for adjusting the pH of the buffer used. The latter was obtained by mixing N-(2-Hydroxyethyl)piperazine-N′-(2-ethanesulfonic acid) and sodium salt (0.01 M HEPES, 0.15 M NaCl, pH 7.4). The OneStep approach [39] was applied to investigate the interactions between immobilized IDE and insulin whose initial concentration was 8 μM. The software Qdat was used to fit the experimental curves according to the equations given in References [39,40]. Briefly, the signal response (R) versus time (t) is given by:

$$dR/dt = k_a * C * R_{max} - (k_a * C + k_d) * R$$

where, C is the analyte concentration, R_{max} is the capacity of immobilized ligand, and k_a and k_d are the kinetic constants. For an injection beginning at time t_0 and ending at t_1, we have:

$$c_1 = C * k_a + k_d.$$

For $t_0 < t < t_1$ (association phase):

$$R(t) = C * k_a * R_{max} * (1 - \exp(-c_1 * (t - t_0)))/c_1.$$

For $t > t_1$ (dissociation phase):

$$R(t) = C * k_a * R_{max} * (1 - \exp(-c_1 * (t_1 - t_0))) / c_1 * \exp(-k_d * (t - t_1)).$$

For multi-site kinetics, the total response is given as the sum of response from each individual site. So for site 1: $R_1(t,k_{a1},k_{d1},R_{max1})$ and site 2: $R_2(t,k_{a2},k_{d2},R_{max2})$, total response $R(t) = R_1 + R_2$. Fitting is performed using standard Levenberg–Marquardt nonlinear least squares optimization, minimizing the sum-squared error of the difference between the model and the experimental data.

3. Results and discussion

In order to evaluate the effect of the pH on IDE activity toward insulin, MS spectra have been acquired as reported in Section 2.1 for solutions containing IDE and insulin at various pH values. The pH of the solutions was adjusted by adding HCl or NaOH, while the reaction time was fixed at 60 min [15]. In Fig. 1 the mass spectra obtained at some representative pH values are reported. It is possible to see that the enzyme is totally inactive at pH 3, as insulin fragments are detected only for solutions having pH ≥ 5, while the enzyme is still active even for pH values as high as 10. Interestingly, apart from the changes on the overall activity, it is possible to note that the insulin fragments detected at alkaline pH are different from the ones detected at physiological pH. Particularly, the insulin fragments involving the C-terminal residues of the insulin A chain [A (14–21) and A (15–21)] and the fragments B (17–24) and

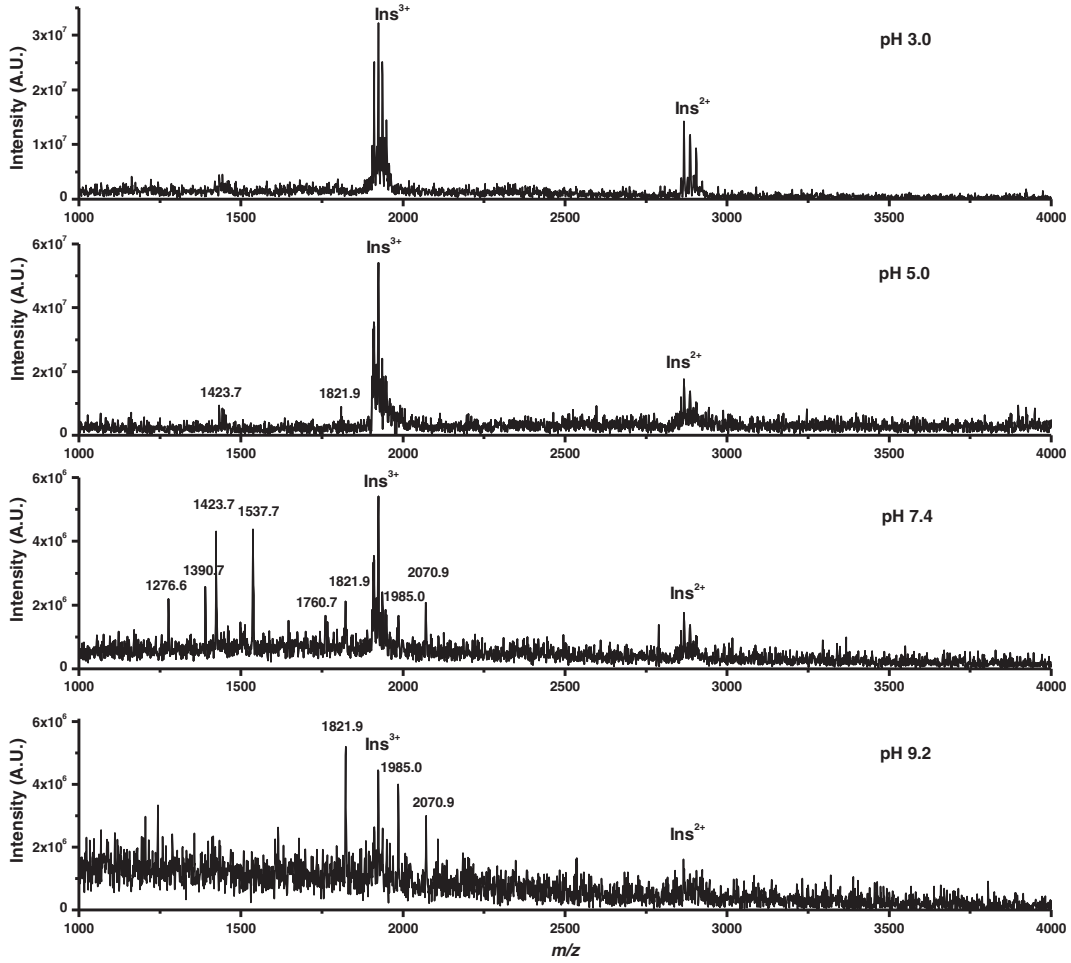

Fig. 1. Mass spectra recorded for solutions containing IDE 20 nM and insulin 10 μM after 1 h incubation at 37 °C at the various pH values indicated. Assignment of the insulin fragments is as reported in Ref. [15].

B (17–25) are mainly produced at alkaline pH [15]. The same set of insulin fragments are known to be produced in solutions containing IDE at high concentrations [15] and therefore it is easy to speculate that the pH, as well as the enzyme concentration, has an effect on IDE oligomerization state, acidic pH shifting the equilibrium toward the monomeric form.

The results of the AFM study on IDE solutions at different pH values are shown in Fig. 2. At pH = 3, the predominant IDE features are small round-shaped aggregates, with an average height of ~0.5 nm, whereas at the pH = 5 stretched fragments start to be visible, with a concurrent growth of the average height to ~0.8 nm. For both the neutral and the basic pH, the measured average height of the enzyme aggregates is ~0.6 nm but the extents of the observed features – especially the coiled structures – spread as the pH increases. The aspect ratio graphs in Fig. 2 clearly display the depicted trends.

According to literature data, each IDE monomer comprises four structurally homologous αβ roll domains (domain 1, residues 43–285;

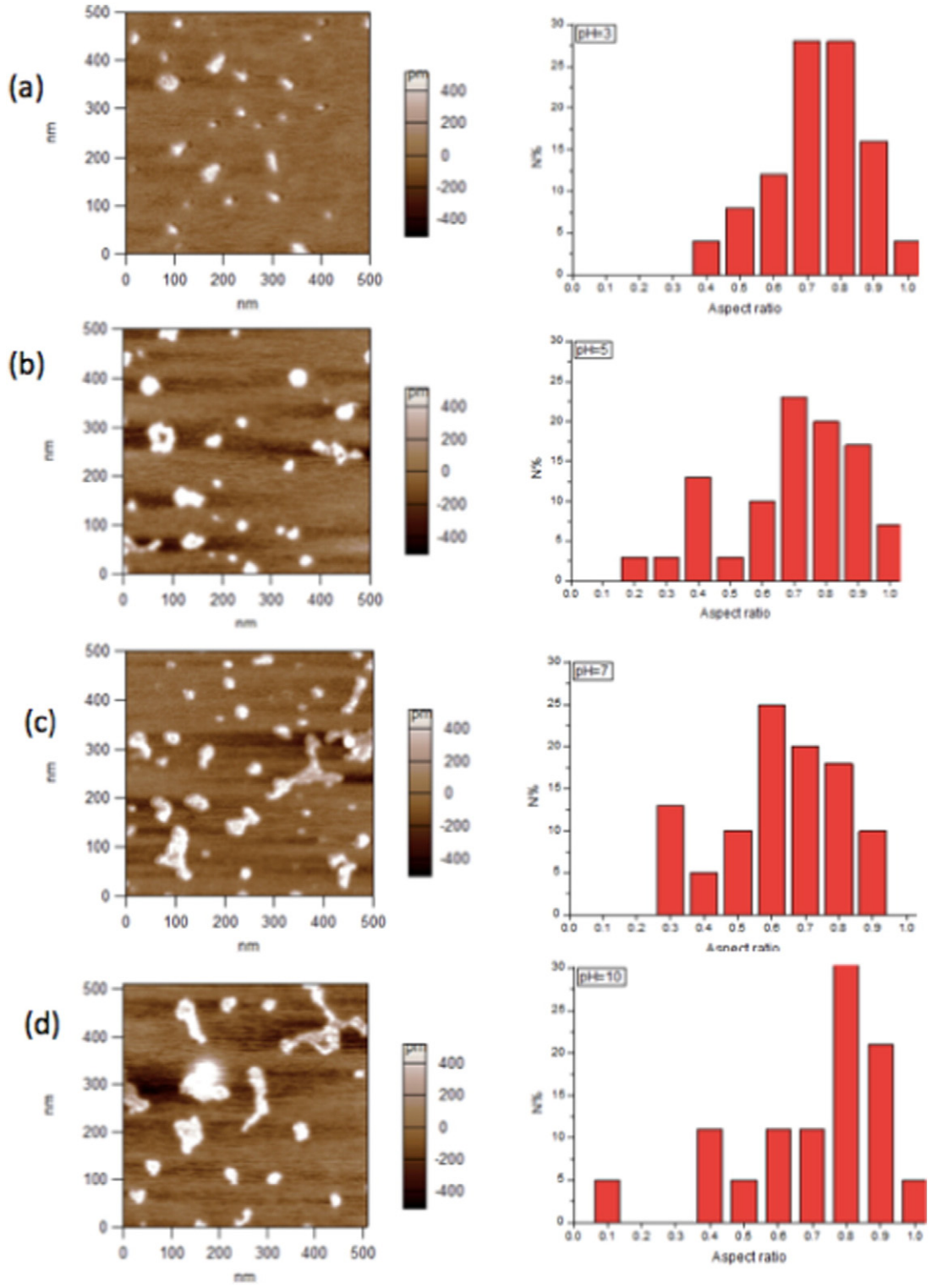

Fig. 2. AC mode in air images of topography on a scan size of 500 nm × 500 nm and measured aspect ratio analyses for IDE deposited on mica from protein solutions at the pH of: (a) 3; (b) 5; (c) 7 and (d) 10.

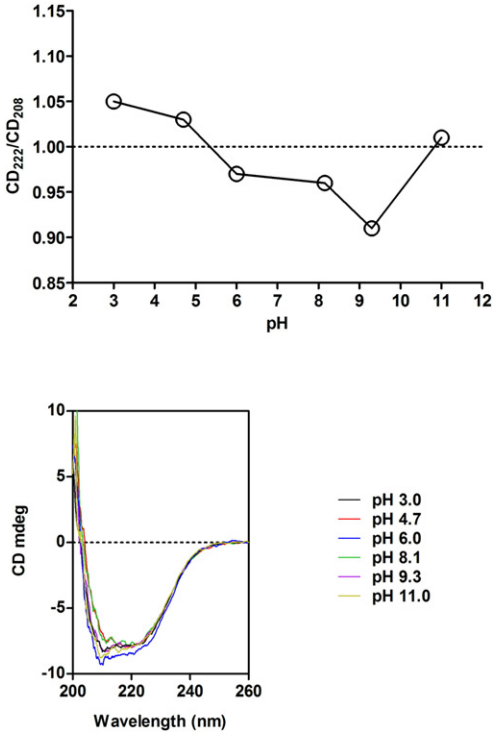

Fig. 3. Lower panel: CD spectra of IDE at different pH values. Upper panel: Plot of the ratio CD_{222}/CD_{208} obtained by spectra of IDE as a function of pH.

domain 2, residues 286–515; domain 3, residues 542–768; and domain 4, residues 769–1016), which share less than 25% sequence similarity. The N-terminal domains 1 and 2 form a αβαβα sandwich (IDE-N), as do domains 3 and 4 (IDE-C) [41]. IDE-N and IDE-C are joined by a 28-residue extended loop and form an enclosed chamber, shaped like a triangular prism, with triangular base dimensions of 3.5 × 3.4 × 3 nm and a height of 3.6 nm. This enclosed cavity has a total volume of ~13 nm [3,42]. The size contraction observed in our samples is explained on the basis of the used experimental conditions, i.e., the air imaging mode and, most importantly, the surface effect of the mica substrates. Indeed, in the spanned pH interval, ranging from the acidic pH = 3 to the basic pH = 10, the enzyme molecules, with an isoelectric pH of 5.8 [43] suffer a widespread effect of charge matching with the mica substrate. The following significant contribution of electrostatic forces at the biointerface might result in changes in viscoelastic and conformational arrangements of the protein adlayer [44]. However, despite these considerations, the observed AFM trends for the IDE aggregates at the different pH values suggest that IDE deposited on mica surfaces tends to increase its volume in basic conditions.

Table 1
Analysis of IDE thermal stability as a function of pH. Fitting of 60 experimental CD_{222} (T) points to a four-parameter logistic equation-sigmoidal curve model. $T_{1/2}$ is the T value when the response is halfway between 0 and 100% of unfolded protein.

	pH 4.7	pH 6	pH 8.15	pH 9.3
Best-fit values				
T1/2	55.19	56.29	61.25	56.66
Std. error				
T1/2	0.399	0.5135	0.8982	0.2785
95% confidence intervals				
T1/2	54.39 to 55.99	55.26 to 57.32	59.45 to 63.05	56.10 to 57.21
Goodness of fit				
R^2	0.9808	0.9833	0.9834	0.9904

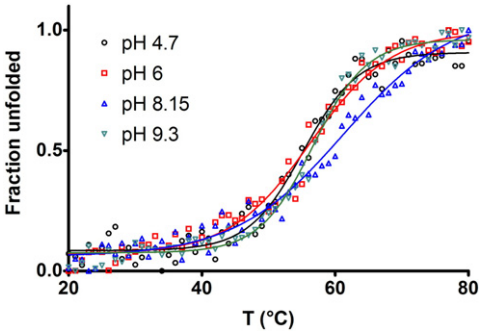

Fig. 4. Normalized CD melting profiles of IDE at different pH values. Heating rate was 1 °C/min for all the experiments.

Lower panel of Fig. 3 reports the far-UV CD spectra of IDE recorded at different pH values and at room temperature. All spectra show two evident absorptions around 220 and 208 nm, and a positive band at wavelengths < 200 nm which are characteristic of α-helical structures. No significant deviations of the CD spectrum are observed in all the investigated pH range, indicating that IDE has a comparable secondary structure at all pH values. Nonetheless, further insights on the effects of pH on IDE structure may be obtained by analyzing the trend of CD_{222}/CD_{208} ratio as a function of pH (Fig. 3, lower panel). It is known that the CD_{222}/CD_{208} ratios <1 are indicative of purely α-helical structures [45]. In contrast, CD spectra showing CD_{222}/CD_{208} ratios >1 are associated with coiled coils or α-helical bundles and assemblies of helical peptides [46]. Our data indicate that IDE may assume a pure α-helical structure at pH values ranging from 6 to 9. By contrast, acidic and severe basic conditions may trigger a conformational transition toward the formation of helix bundles. The effect of pH variations on the thermal stability of IDE was also investigated by CD at different temperatures. This technique has the advantage of a lower usage of sample if compared to Differential Scanning Calorimetry [47,48]. The melting temperature values (Table 1) were determined from the CD melting profiles for IDE monitored at 222 nm with a heating rate of 1 °C/min (Fig. 4). The CD melting curves evidence that, at neutral pH, IDE exhibits the greatest thermal stability. It is worthy to remind that IDE adopts a purely α-helical conformation at neutral pH and a coiled coil structure in basic conditions.

To improve our understanding of the conformational and/or oligomerization transitions that occur for IDE at different pH values, we surmised that it may be possible to monitor the changes in the

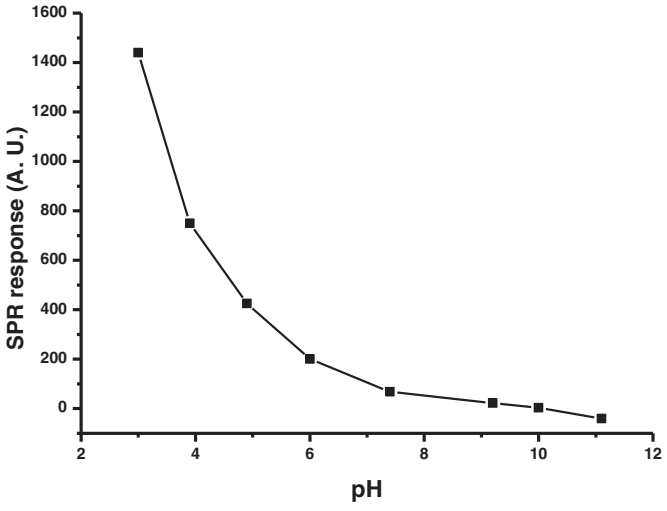

Fig. 5. SPR signal recorded for immobilized IDE at different pH values. Flowing rate of the buffer was 100 μL/min. Solid line is drawn to guide the eyes.

hydrodynamic radius of the enzyme using label free methods. Large scale protein conformational changes can be observed using surface plasmon resonance (SPR). For example, SPR was previously utilized to observe the conformational changes or unfolding that results from urea-induced unfolding of immobilized luciferase, lysozyme, and RNase proteins [49,50]. However, it has been reported that the potential origins of shifts in the angle of SPR can be numerous and tricky, so, before assigning SPR shifts to pH induced conformational changes, one should take into account all the factors that may affect the properties of the bulk solution, the carboxymethyldextran (CMD) layer and the immobilized biomolecule at the sensor surface. Besides pH, these factors include temperature, flow rate, refractive index, and ionic strength of the solution, each of which must be carefully regulated if accurate assignments are to be made and definitive information on the capabilities of SPR for the detection of protein conformational changes obtained [51]. Indeed, once those factors are controlled, the SPR signal is dependent on the refractive index and changes in the dielectric medium in the immediate vicinity of the protein bound to the sensor surface. Enzyme conformational changes and/or oligomerization of the enzyme cause changes in the local water structure and hence in the refractive index. In Fig. 5 the SPR signal recorded for immobilized IDE at different pH values is reported after subtraction of the SPR signal recorded for a bare CMD layer in the same experimental conditions.

Table 2
Kinetic parameters obtained fitting the curves reported in Fig. 6. While for pH ≥ 5.3 the two binding site model is necessary to fit the experimental sensorgram, at pH < 5 the one binding site model has been used, producing a single K_D value. Discussion is in the text.

pH	k_a	k_d	R_{max}	K_D	Res sd
3.0–4.5	8.1×10^2	2.0×10^{-1}	1.66×10^3	250 μM	3.738
5.3	5.0×10^4	1.2×10^{-2}	1.80×10^1	0.2 μM	1.347
	2.3×10^3	1.2×10^{-1}	2.02×10^1	52.4 μM	1.347
7.4	1.3×10^4	5.1×10^{-3}	4.21×10^1	0.4 μM	5.582
	2.9×10^3	9.0×10^{-2}	9.0×10^2	31 μM	5.582
9.0	2.1×10^4	3.6×10^{-3}	1.91×10^1	0.2 μM	1.651
	1.8×10^4	4.0×10^{-2}	6.80×10^1	2.3 μM	1.651
10.0	2.0×10^3	1.1×10^{-3}	8.0×10^1	0.5 μM	1.499
	1.0×10^3	4.6×10^{-2}	5.0×10^2	100 μM	1.499

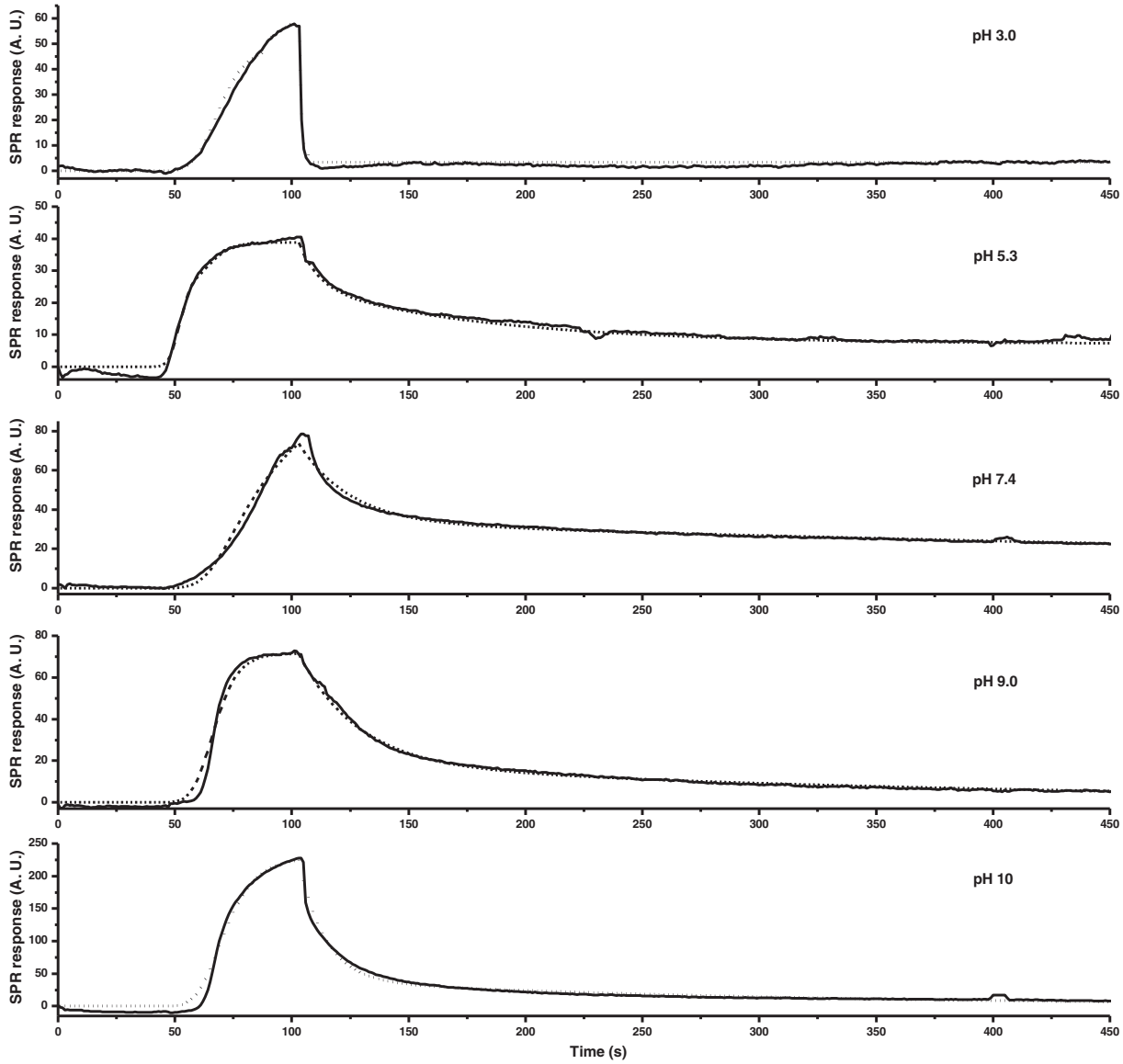

Fig. 6. SPR sensorgrams obtained experimentally (solid lines) for immobilized IDE and insulin flowing solutions (8 μM, OneStep mode) at the pH indicated. Simulation (dashed lines) has been obtained by using the fitting model described in Section 2.4. Please note that in the case of pH = 3 one binding site model was used, while for all the other pH values the two binding site model was necessary to fit the experimental curves.

It is important to highlight that within the pH range reported in Fig. 5 (3–11), the SPR response was reproducible in our experimental conditions, that is the same values were recorded independently from the order at which the immobilized IDE got in contact with the solutions at different pH values. This reproducibility proves that the changes in the SPR baseline are not due to irreversible degradation of the CMD layer, which indeed occurs in our experimental conditions outside the indicated pH range [51]. Moreover, the same experiment was performed with immobilized albumin and the large increase of SPR response for acidic pH was not observed (data not reported). The large SPR response obtained for IDE at acidic pH is here attributed to a change in the enzyme conformation. However, we are aware that it is not straightforward to interpret the large SPR signal obtained at acidic pH as a conformational change of the enzyme, as this could be simply due to a larger electrostatic interaction of the enzyme for the negatively charged CMD layer below IDE isoelectric point (5.8) [43]. For this reason, we have performed another SPR experiment where the interaction of IDE with insulin was monitored in real time at different pH values. In Fig. 6 the SPR sensorgrams are shown while in Table 2 the kinetic parameters obtained by fitting the experimental curves as described in Section 2.4 are also reported. It is important to highlight that while at pH ≥ 5.3 it was necessary to use the two binding site model in order to fit the experimental sensorgrams, in the case of pH < 5, the one binding site model was able to produce a good fitting of the experimental curves. It is known that IDE binds its long substrates (insulin, Aβ, etc.) through two anchoring sites, namely the catalytic site and the exosite that is at about 30 Å away [5]. Our SPR results indicate that at very low pH (<5) IDE loses its capability to bind insulin at the catalytic site, so that the substrate is quickly released (see Table 2) and fragments are not formed, as assessed by the MS investigation reported above.

4. Conclusions

In this work we have investigated the effect of different pH values on IDE conformation and oligomerization state as well as on IDE capability to bind and degrade insulin molecules. We have found that IDE undergoes conformational and oligomeric changes that occur in a gradual mode over the pH range scrutinized (3–11). SPR results indicate that insulin binds IDE only at one anchoring site at acidic pH, while two binding sites have to be considered to fit the experimental SPR curves obtained for the insulin–IDE interaction at neutral and basic pH. MS results confirm that such different binding features affect IDE capability to degrade insulin, as the enzyme is inactive toward the hormone at acidic pH. Moreover, the insulin fragments detected by MS at basic pH involve the C-terminal residues of the insulin A chain [A (14–21) and A (15–21)] and the fragments B (17–24) and B (17–25). The same set of insulin fragments are known to be produced in solutions containing IDE at high concentrations, where the equilibrium in the oligomerization state of the enzyme is mainly shifted toward the dimeric and/or tetrameric forms. These results indicate that IDE has a different conformation at acidic pH that shifts the oligomeric equilibrium toward the monomeric form. AFM study confirmed that IDE molecules increase their volume in basic conditions, while analysis of the CD data concerning IDE thermal denaturation and pH titration provided further insights into the role of ionic interactions to the enzyme overall stability and conformational dynamics. IDE thermal stability exhibited a significant immunity to pH perturbation in the 3 < pH < 10 range, while conformational alterations at extreme pH values appear to be associated with the formation of coiled coil structures. The demonstrated low sensitivity of the protein melting temperature to pH variations suggests that native ionic interactions do not play a predominant role to the stabilization of IDE. On the other hand, our results indicate that disruption of the native ionic contacts may interfere with IDE oligomerization and results in a prompt inactivation of the enzyme. Therefore if on one hand pH was shown to have poor influence on IDE stability thus suggesting a high degree of structural plasticity of this protein, on the other hand it is crucial for ensuring the functional integrity of IDE in that pH variations invariably result in changes of the oligomerization state and enzyme inactivation, even in conditions that do not disrupt the general topology of the protein.

It has been reported that IDE is expressed in several different tissues as well as being located in various cellular compartments [33] that experience different pH values. Our results show that IDE capability to bind and degrade insulin molecules, as well as the cryptic peptides generated by the action of the enzyme on insulin, are strongly dependent on the pH. It is important to highlight that diabetic ketoacidosis is a potentially life-threatening complication in patients with diabetes mellitus, resulting from a shortage of insulin in response to which the body switches to burning fatty acids and producing acidic ketone bodies that cause most of the symptoms and complications. Here we have demonstrated that cellular acidosis can also have a large effect on IDE oligomerization state, inducing an enzyme inactivation and an altered insulin degradation that could have an impact on insulin signaling.

Acknowledgment

We thank FIRB “RINAME” RBAP114AMK and PRIN 2008R23Z7K for partial financial support.

References

[1] H. Fakhrai-Rad, A. Nikoshkov, A. Kamel, M. Fernstrom, J.R. Zierath, S. Norgren, H. Luthman, J. Galli, Insulin-degrading enzyme identified as a candidate diabetes susceptibility gene in GK rats, Hum. Mol. Genet. 9 (2000) 2149–2158.
[2] G.R. Tundo, D. Sbardella, C. Ciaccio, A. Bianculli, A. Orlandi, M.G. Desimio, G. Arcuri, M. Coletta, S. Marini, Insulin-degrading enzyme (IDE): a novel heat shock-like protein, J. Biol. Chem. 288 (2013) 2281–2289.
[3] A. Fernandez-Gamba, M.C. Leal, L. Morelli, E.M. Castano, Insulin-degrading enzyme: structure–function relationship and its possible roles in health and disease, Curr. Pharm. Des. 15 (2009) 3644–3655.
[4] C. Ciaccio, G.R. Tundo, G. Grasso, G. Spoto, D. Marasco, M. Ruvo, M. Gioia, E. Rizzarelli, M. Coletta, Somatostatin: a novel substrate and a modulator of insulin-degrading enzyme activity, J. Mol. Biol. 385 (2009) 1556–1567.
[5] M. Manolopoulou, Q. Guo, E. Malito, A.B. Schilling, W.J. Tang, Molecular basis of catalytic chamber-assisted unfolding and cleavage of human insulin by human insulin-degrading enzyme, J. Biol. Chem. 284 (2009) 14177–14188.
[6] N. Noinaj, S.K. Bhasin, E.S. Song, K.E. Scoggin, M.A. Juliano, L. Juliano, L.B. Hersh, D.W. Rodgers, Identification of the allosteric regulatory site of insulysin, PLoS ONE 6 (2011) e20864.
[7] L.A. McCord, W.G. Liang, E. Dowdell, V. Kalas, R.J. Hoey, A. Koide, S. Koide, W.-J. Tang, Conformational states and recognition of amyloidogenic peptides of human insulin-degrading enzyme, Proc. Natl. Acad. Sci. U. S. A. 110 (2013) 13827–13832.
[8] G. Grasso, E. Rizzarelli, G. Spoto, How the binding and degrading capabilities of insulin degrading enzyme are affected by ubiquitin, Biochim. Biophys. Acta Protein Proteomics 1784 (2008) 1122–1126.
[9] O. Amata, T. Marino, N. Russo, M. Toscano, Human insulin-degrading enzyme working mechanism, J. Am. Chem. Soc. 131 (2009) 14804–14811.
[10] S.O. Abdul-Hay, A.L. Lane, T.R. Caulfield, C. Claussin, J. Bertrand, A. Masson, S. Choudhry, A.H. Fauq, G.M. Maharvi, M.A. Leissring, Optimization of peptide hydroxamate inhibitors of insulin-degrading enzyme reveals marked substrate-selectivity, J. Med. Chem. 56 (2013) 2246–2255.
[11] C. Cabrol, M.A. Huzarska, C. Dinolfo, M.C. Rodriguez, L. Reinstatler, J. Ni, L.-A. Yeh, G.D. Cuny, R.L. Stein, D.J. Selkoe, M.A. Leissring, Small-molecule activators of insulin-degrading enzyme discovered through high-throughput compound screening, PLoS ONE 4 (2009) e5274.
[12] S.O. Abdul-Hay, D. Kang, M. McBride, L. Li, J. Zhao, M.A. Leissring, Deletion of insulin-degrading enzyme elicits antipodal, age-dependent effects on glucose and insulin tolerance, PLoS ONE 6 (2011) e20818.
[13] M.A. Leissring, The AβCs of Aβ-cleaving proteases, J. Biol. Chem. 283 (2008) 29645–29649.
[14] E.S. Song, A. Daily, M.G. Fried, M.A. Juliano, L. Juliano, L.B. Hersh, Mutation of active site residues of insulin-degrading enzyme alters allosteric interactions, J. Biol. Chem. 280 (2005) 17701–17706.
[15] G. Grasso, E. Rizzarelli, G. Spoto, The proteolytic activity of insulin-degrading enzyme: a mass spectrometry study, J. Mass Spectrom. 44 (2009) 735–741.
[16] E.S. Song, D.W. Rodgers, L.B. Hersh, Mixed dimers of insulin-degrading enzyme reveal a cis activation mechanism, J. Biol. Chem. 286 (2011) 13852–13858.
[17] G. Grasso, F. Salomone, G.R. Tundo, G. Pappalardo, C. Ciaccio, G. Spoto, A. Pietropaolo, M. Coletta, E. Rizzarelli, Metal ions affect insulin-degrading enzyme activity, J. Inorg. Biochem. 117 (2012) 351–358.
[18] G. Grasso, A. Pietropaolo, G. Spoto, G. Pappalardo, G.R. Tundo, C. Ciaccio, M. Coletta, E. Rizzarelli, Copper(I) and copper(II) inhibit Aβ peptides proteolysis by insulin-

degrading enzyme differently: implications for metallostasis alteration in Alzheimer's disease, Chem. Eur. J. 17 (2011) 2752–2762.
[19] F. Bellia, A. Pietropaolo, G. Grasso, Formation of insulin fragments by insulin-degrading enzyme: the role of zinc(II) and cystine bridges, J. Mass Spectrom. 48 (2013) 135–140.
[20] F. Bellia, G. Grasso, The role of copper(II) and zinc(II) in the degradation of human and murine IAPP by insulin-degrading enzyme, J. Mass Spectrom. 49 (2014) 274–279.
[21] R. Wang, S. Wang, J.S. Malter, D.-S. Wang, Effects of 4-hydroxy-nonenal and amyloid-β on expression and activity of endothelin converting enzyme and insulin degrading enzyme in SH-SY5Y cells, J. Alzheimers Dis. 17 (2009) 489–501.
[22] L.A. Ralat, M. Ren, A.B. Schilling, W.J. Tang, Protective role of Cys-178 against the inactivation and oligomerization of human insulin-degrading enzyme by oxidation and nitrosylation, J. Biol. Chem. 284 (2009) 34005–34018.
[23] M. Neant-Fery, R.D. Garcia-Ordoñez, T.P. Logan, D.J. Selkoe, L. Li, L. Reinstatler, M.A. Leissring, Molecular basis for the thiol sensitivity of insulin-degrading enzyme, Proc. Natl. Acad. Sci. U. S. A. 105 (2008) 9582–9587.
[24] W.C. Duckworth, R.G. Bennett, F.G. Hamel, Insulin degradation: progress and potential, Endocr. Rev. 19 (1998) 608–624.
[25] W.L. Kuo, B.D. Gehm, M.R. Rosner, W. Li, G. Keller, Inducible expression and cellular localization of insulin-degrading enzyme in a stably transfected cell line, J. Biol. Chem. 269 (1994) 22599–22606.
[26] F. Authier, B.I. Posner, J.J. Bergeron, Insulin-degrading enzyme, Clin. Invest. Med. 19 (1996) 149–160.
[27] W. Farris, M.A. Leissring, M.L. Hemming, A.Y. Chang, D.J. Selkoe, Alternative splicing of human insulin-degrading enzyme yields a novel isoform with a decreased ability to degrade insulin and amyloid beta-protein, Biochemistry 44 (2005) 6513–6525.
[28] K.A. Seta, R.A. Roth, Overexpression of insulin degrading enzyme: cellular localization and effects on insulin signalling, Biochem. Biophys. Res. Commun. 231 (1997) 167–171.
[29] J.A. Lynch, A.M. George, P.B. Eisenhauer, K. Conn, W. Gao, I. Carreras, J.M. Wells, A. McKee, M.D. Ullman, R.E. Fine, Insulin degrading enzyme is localized predominantly at the cell surface of polarized and unpolarized human cerebrovascular endothelial cell cultures, J. Neurosci. Res. 83 (2006) 1262–1270.
[30] M. Grabe, G. Oster, Regulation of organelle acidity, J. Gen. Physiol. 117 (2001) 329–343.
[31] Y. Su, P.-T. Chang, Acidic pH promotes the formation of toxic fibrils from β-amyloid peptide, Brain Res. 893 (2001) 287–291.
[32] A.L. Pey, pH-dependent relationship between thermodynamic and kinetic stability in the denaturation of human phosphoglycerate kinase 1, Biochimie 103 (2014) 7–15.
[33] L.B. Hersh, The insulysin (insulin degrading enzyme) enigma, Cell. Mol. Life Sci. 63 (2006) 2432–2434.
[34] J.R. Casey, S. Grinstein, J. Orlowski, Sensors and regulators of intracellular pH, Nat. Rev. Mol. Cell Biol. 11 (2010) 50–61.
[35] E. Padan, E. Bibi, M. Ito, T.A. Krulwich, Alkaline pH homeostasis in bacteria: new insights, Biochim. Biophys. Acta 1717 (2005) 67–88.
[36] G. Grasso, A.I. Bush, R. D'Agata, E. Rizzarelli, G. Spoto, Enzyme solid-state support assays: a surface plasmon resonance and mass spectrometry coupled study of immobilized insulin degrading enzyme, Eur. Biophys. J. 38 (2009) 407–414.
[37] G. Grasso, M. Fragai, E. Rizzarelli, G. Spoto, K.J. Yeo, A new methodology for monitoring the activity of cdMMP-12 anchored and freeze-dried on Au (111), J. Am. Soc. Mass Spectrom. 18 (2007) 961–969.
[38] G. Grasso, P. Mielczarek, M. Niedziolka, J. Silberring, Metabolism of cryptic peptides derived from neuropeptide FF precursors: the involvement of insulin-degrading enzyme, Int. J. Mol. Sci. 15 (2014) 16787–16799.
[39] J.G. Quinn, Evaluation of Taylor dispersion injections: determining kinetic/affinity interaction constants and diffusion coefficients in label-free biosensing, Anal. Biochem. 421 (2012) 401–410.
[40] D.J. O'Shannessy, M. Brigham-Burke, K.K. Soneson, P. Hensley, I. Brooks, Determination of rate and equilibrium binding constants for macromolecular interactions using surface plasmon resonance: use of nonlinear least squares analysis methods, Anal. Biochem. 212 (1993) 457–468.
[41] P. Li, W.-L. Kuo, M. Yousef, M.R. Rosner, W.-J. Tang, The C-terminal domain of human insulin degrading enzyme is required for the dimerization and substrate recognition, Biochem. Biophys. Res. Commun. 343 (2006) 1032–1037.
[42] Y. Shen, A. Joachimiak, M.R. Rosner, W.-J. Tang, Structures of human insulin-degrading enzyme reveal a new substrate recognition mechanism, Nature 443 (2006) 870–874.
[43] H.J. Kolb, E. Standl, Purification to homogeneity of an insulin-degrading enzyme from human erythrocytes, Hoppe Seylers Z. Physiol. Chem. 361 (1980) 1029–1039.
[44] C. Satriano, S. Svedhem, B. Kasemo, Well-defined lipid interfaces for protein adsorption studies, Phys. Chem. Chem. Phys. 14 (2012) 16695–16698.
[45] S.Y. Lau, A.K. Taneja, R.S. Hodges, Synthesis of a model protein of defined secondary and quaternary structure. Effect of chain length on the stabilization and formation of two-stranded a-helical coiled-coils, J. Biol. Chem. 259 (1984) 13253–13261.
[46] K. Dutta, A. Alexandrov, H. Huang, S.M. Pascal, pH-induced folding of an apoptotic coiled coil, Protein Sci. 10 (2001) 2531–2540.
[47] M. Pappalardo, D. Milardi, D. Grasso, C. La Rosa, Phase behaviour of polymer-grafted DPPC membranes for drug delivery systems design, J. Therm. Anal. Calorim. 80 (2005) 413–418.
[48] D. Grasso, C. La Rosa, D. Milardi, S. Fasone, The effects of scan rate and protein concentration on DSC thermograms of bovine superoxide dismutase, Thermochim. Acta 265 (1995) 163–175.
[49] L.Y. Chen, Monitoring conformational changes of immobilized RNase A and lysozyme in reductive unfolding by surface plasmon resonance, Anal. Chim. Acta 631 (2009) 96–101.
[50] T. Zako, K. Harada, T. Mannen, S. Yamaguchi, A. Kitayama, H. Ueda, T. Nagamune, Monitoring of the refolding process for immobilized firefly luciferase with a biosensor based on surface plasmon resonance, J. Biochem. 129 (2001) 1–4.
[51] S. Paynter, D.A. Russell, Surface plasmon resonance measurement of pH-induced responses of immobilized biomolecules: conformational change or electrostatic interaction effects? Anal. Biochem. 309 (2002) 85–95.